Thin-Film HTS Planar Antennas

Michael J. Lancaster, *Member, IEEE*, Hanyang Y. Wang, and Jia-Sheng Hong, *Member, IEEE*
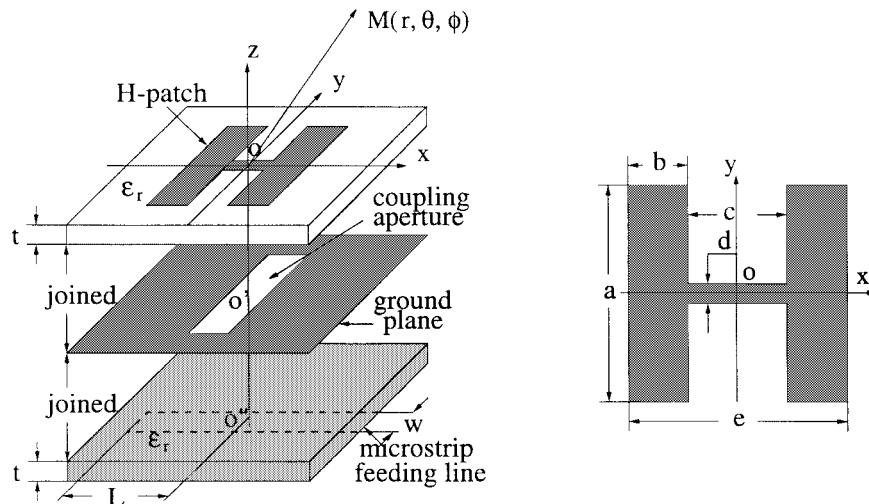

Fig. 1. The "H" antenna and feed network. The dimensions of the antenna used in the examples below are $a = 5.5$ mm, $b = 1.5$ mm, $c = 2.5$ mm, and $d = 0.5$ mm, and the aperture is 5.5 by 2.5 mm. For the copper antenna $t = 1.27$ mm, $\varepsilon_r = 10.8$, and for the YBCO superconducting antenna the upper substrate has $t = 1$ mm and $\varepsilon_r = 9.8$.

Abstract— The "H" microstrip antenna is suitable for use as an efficient small antenna when it is constructed out of superconducting thin-film materials. An aperture feed and matching network is described which provides a convenient enhancement of the capabilities of the "H" antenna. Methods of prediction of the center frequency are given. In addition, an analytical expression is developed for the farfield radiation pattern of the "H" antenna and the efficiency and Q of superconducting and copper antennas are described using this expression. It is likely that superconducting antennas will only have significant application when they are used in arrays. Three arrays are described demonstrating multiband self-diplexing multifrequency-enhanced bandwidth and multifrequency beam forming.

Index Terms— High-temperature conductors, patch antenna, superconductor.

I. INTRODUCTION

A SUPERCONDUCTING antenna was one of the first microwave components to be demonstrated as an application of high-temperature superconducting material [1]. Since then, there has been considerable work on new types of superconducting antennas, with patch antennas looking like an interesting possibility for a number of applications [2]–[7].

The advantage of using superconducting materials in the development of antennas is the increase in efficiency or

gain. There are a number of ways for this improvement in efficiency to occur [2]: 1) For small antennas, the power losses in the metallic parts of conventional metallic antennas can dominate over the power radiated. Hence reducing these losses by using a low surface resistance material, such as a superconductor, increases the efficiency. 2) Losses are not only important in the antenna element itself, but also the losses in the matching network can contribute to the overall efficiency. A superconducting matching network reduces the matching network loss. 3) Superdirectional antenna arrays become more efficient with the use of superconductors [2]. 4) In complex high-frequency (> 20 GHz) arrays, losses in the feed network may contribute to reduced efficiency, but making the network out of superconductors effectively removes this problem. and 5) There are now many applications, other than antennas, in which superconductors are used. Integrating antennas with additional functionality within these systems can offer significant additional benefits.

A potential problem for electrically small and superdirective antennas is the high radiation quality factor which together with high efficiency, in the case of superconductive realization, results in narrow bandwidth operation. This is due to the low loss superconducting materials and the difficulty of designing and constructing potentially complex matching networks. The cooling requirements are of course a problem to practical implementation, but cooler technology has improved vastly over the last few years and will continue to do so. The additional power requirement required by the cooler must of course be considered carefully for any application. The power-
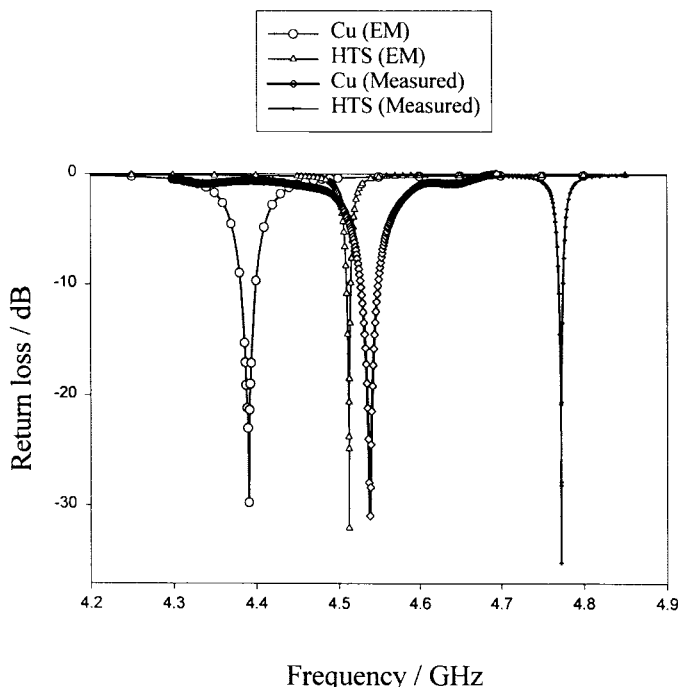
Fig. 2. Return loss as a function of frequency for copper and HTS antennas compared with the full-wave simulation.

Fig. 3. Experimental results of the resonant frequency of the "H" antenna compared with different methods of analysis. The antennas are square, and with the length and width shown on the ordinate they have $a/b = 3.67$, $a/c = 2.2$, $a/d = 11.0$ $a/e = 1$.

handling capability of the superconducting material may also be of concern for high-power transmit applications.

This paper addresses some of the perceived problems with superconducting antennas. Firstly, the "H" antenna is studied in detail with new analytical expressions developed for its performance. This antenna has a simple feed and matching network. Arrays of this antenna type are demonstrated which show the flexibility and the multifunctionality of the structure; methods of increasing the bandwidth are also demonstrated. Planar arrays with capabilities of filtering, dual polarization, circular or elliptical polarization, self-duplexing, and multifrequency operation are discussed.

II. The "H" Antenna

The "H" antenna shown in Fig. 1 was first demonstrated in 1985 [8], and it has been investigated in its superconducting form for a number of years [9]–[12]. The feed networks for the early antennas were coaxial cables. However, more recently an aperture-fed version has been demonstrated [13], [14]. This is far more suitable for implementation in arrays [15]. The miniaturization of the antenna comes about from both the shape of the "H" element and the high dielectric constant of the substrate on which it is placed.

A. Aperture Feed

The aperture coupled "H" antenna shown in Fig. 1 consists of two dielectric layers and three metallic layers. On the bottom of the lower dielectric substrate is the microstrip feed network, shown as the dotted line in the figure. The ground plane for this microstrip is on the upper side of the lower dielectric. In Fig. 1 this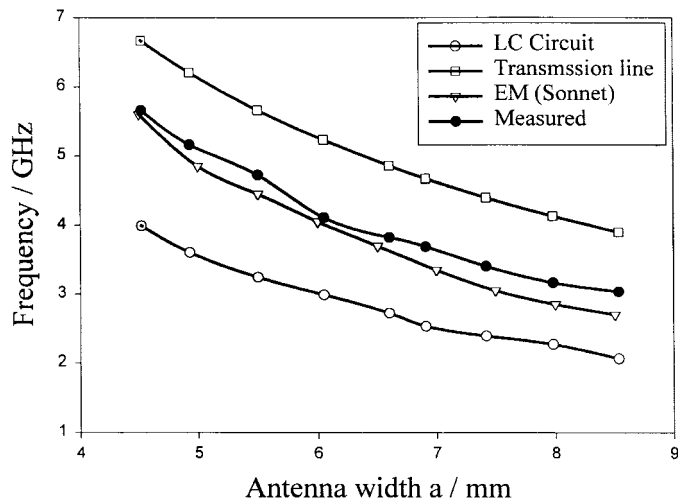 is separated from the dielectric for clarity. This ground plane has a rectangular aperture cut into it; this is the coupling aperture. The "H" antenna is patterned onto the upper surface of the upper dielectric and energy is coupled to it through the aperture. The aperture resonance frequency is much higher than the resonance frequency of the "H" patch. Matching is achieved by the correct positioning of the "H" over the aperture and adjusting the length L of the microstrip which extends beyond the aperture.

There are a number of distinct advantages of having this particular type of structure, where the patch is isolated from the feed network: 1) there is no spurious radiation from the feed; 2) the substrate can be a different material from the feed; 3) the implementation of the matching circuit is straightforward; 4) because of the additional area available complex feed networks can be produced; and 5) the symmetrical nature of the feeding structure will result in lower cross polarization in comparison with conventional probe or edge fed microstrip antennas.

The caption for Fig. 1 gives the dimensions of an example antenna used for experimental and theoretical results in the sections below. In the case of the copper antenna, it is produced on RT-Duroid 6010. The superconducting $YBa_2Cu_3O_7$ (YBCO) antennas are produced by laser ablation on MgO substrates. The surface resistance used on the theoretical graphs are [2] 8.7 mΩ for copper at 77 K, 0.1 mΩ for YBCO, and 26.1 mΩ for copper at 300 K. All these values are at a frequency of 10 GHz.

To investigate the resonant properties of the H-shaped patch antennas and examine the differences between the copper patch and high temperature superconductor (HTS) patch antennas, we have simulated and measured the antennas using full-wave analysis (Sonnet Software *em*) and an HP network analyzer. The return loss as a function of frequency for both copper and HTS antennas is shown in Fig. 2. The dimensions of the H-shaped patches are the same as those given in Fig. 1. If allowance is made for fabrication and measurement error,
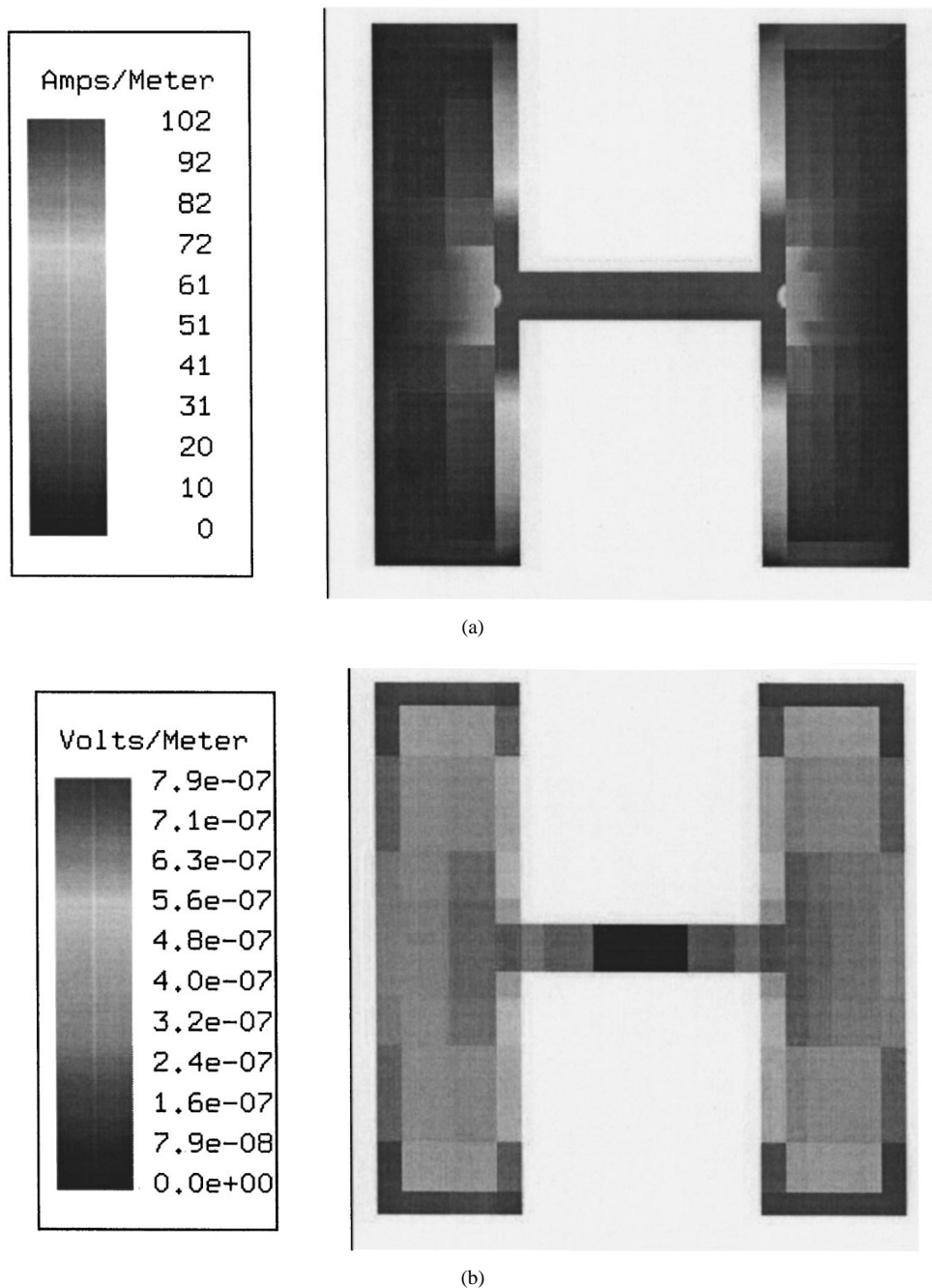
(a)

(b)

Fig. 4.   (a) Current distribution and (b) charge distribution on the "H" antenna with the dimensions given in the caption of Fig. 1.

the agreement between predicated and measured is good. The matching of the antenna is excellent. In comparison with the copper patch, the resonant frequency for the HTS patch is slightly higher. This is attributed to the lower relative dielectric constant of MgO.

B. Resonance Frequency

There are a number of different ways to estimate the resonance frequency of the antenna. Three ways are described below, ranging from a very simple model to the use of full wave analysis software. The results from each of the models are plotted in Fig. 3 and compared with experimental results.

It is possible just to consider the "H" antenna as a simple lumped element circuit, with a capacitance and inductance in series. The resonance frequency of this LC circuit can then be determined. Expressions for the capacitance of a patch and the inductance of a narrow piece of transmission line are available in the literature [16]. This simple model gives the results shown in Fig. 3, and these are compared with the other models and a set of experimental results. Measurements are of 16 antennas each of a different size.

If a straight piece of transmission line is an open circuit at both ends, it behaves as a resonator, with a resonance frequency corresponding to the length of the transmission line being a half wavelength. The "H" antenna can be approxi-
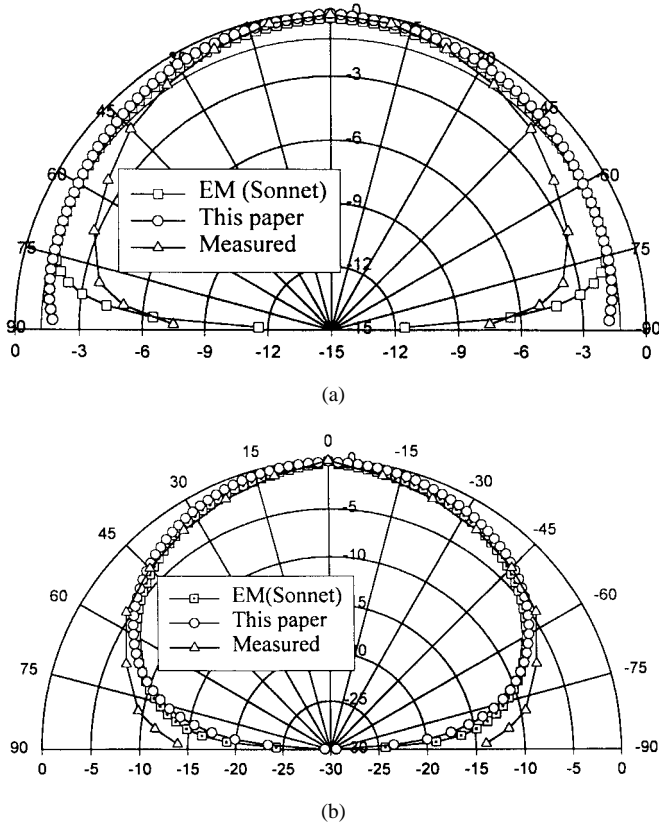
(a)

(b)

Fig. 5.   Radiation patterns of an "H" antenna using (3) and (5)–(7) compared with the radiation pattern calculated using full wave analysis and experimental results. (a) $|\underline{E}|$ in E plane ($\phi = 0°$). (b) $|\underline{E}|$ in H plane ($\phi = 90°$).

mately described in a similar manner, but with dimension e (in Fig. 1) being the length of transmission line. However, the large changes in width of this transmission line affect the effective overall length of the line, as does the field overlap at both of the ends and edges. Both these effects can be taken into account using simple expressions derived in the literature [16]. In equivalent circuit terms, the "H" shape is sometimes called a "stepped impedance resonator." The results of this model are also shown in Fig. 3. Standard microwave design packages use a similar technique and can be used to predict the frequency of operation of the antenna. An alternative method for calculating the resonance frequency of the antenna is to consider it as a short transmission line loaded with two short stubs at each end. This method is described further in [15].

Finally, full wave analysis software can be used to describe the antenna, the aperture, and the feed network. Using Sonnet Software *em*, an accurate prediction of the frequency is obtained as shown in Fig. 3. It is interesting to look at the current and charge distributions on the "H" antenna at resonance and these are shown in Fig. 4.

C. Radiation Pattern

The radiation pattern of a microstrip patch antenna can be calculated by using equivalent sources of magnetic current on the region of dielectric which bounds the antenna structure [17]. This magnetic current, $\underline{M}$, can be calculated from the
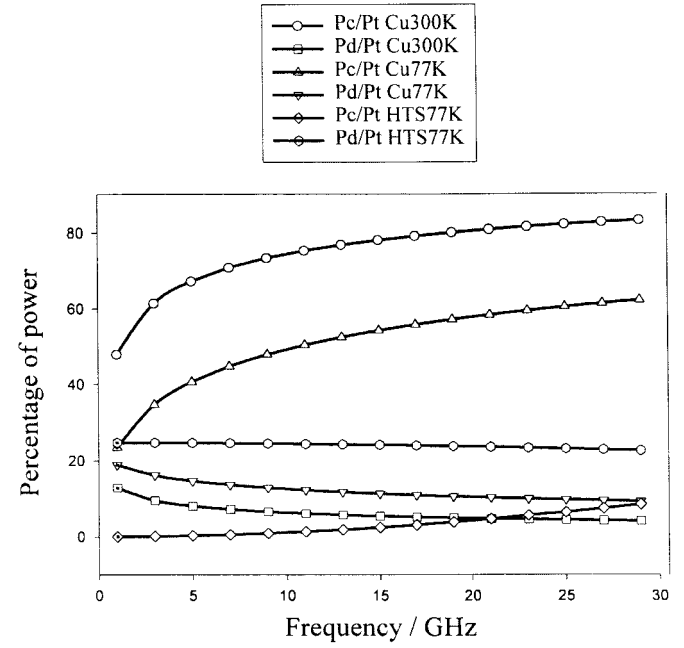

Fig. 6.   Power losses in the "H" antenna using (8) and (9) for the dielectric and conductor losses, respectively. The losses are shown as a percentage of the total loss. The loss tangent for the dielectric used is 10^{-5}.
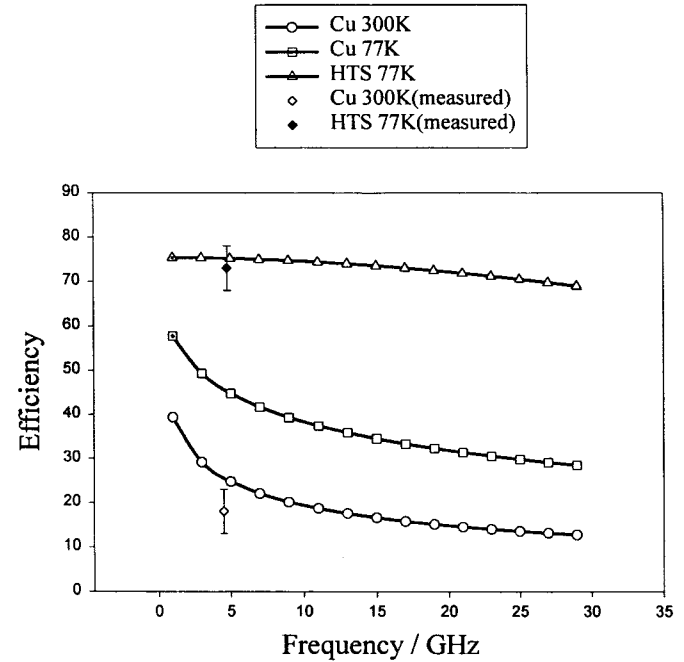

Fig. 7.   Efficiency of copper antennas at 300 K and 77 K compared with a superconducting antenna at 77 K using (11), (10), (6), and (7). The loss tangent for the substrate is 10^{-5}. Experimental results for copper and superconducting antennas are also shown.

electric field in the dielectric on the antenna boundary and its image in a ground plane, which is assumed to be of infinite extent

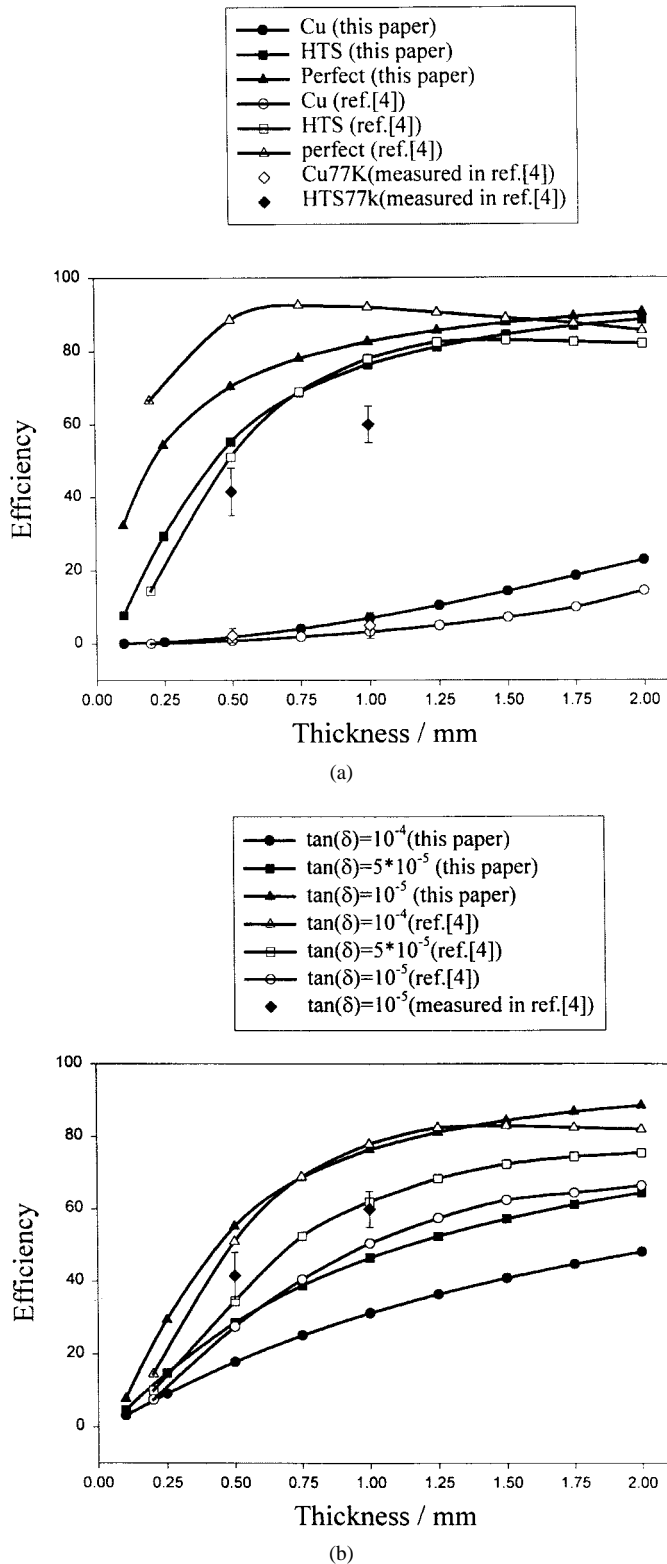$$\underline{M} = 2\underline{E}_t \times \underline{n}. \tag{1}$$

Fig. 8. Comparison of antenna efficiency against substrate thickness for (a) different conducting materials and (b) different loss tangents. Experimental results and full wave analysis using the method of moments are included from [9] and compared with (11) using (6) and (7).

Here $\underline{n}$ is the unit normal to the boundary and $\underline{E}_t$ is the z directed electric field on the boundary. The equivalent magnetic current is therefore directed around the boundary of the antenna patch.
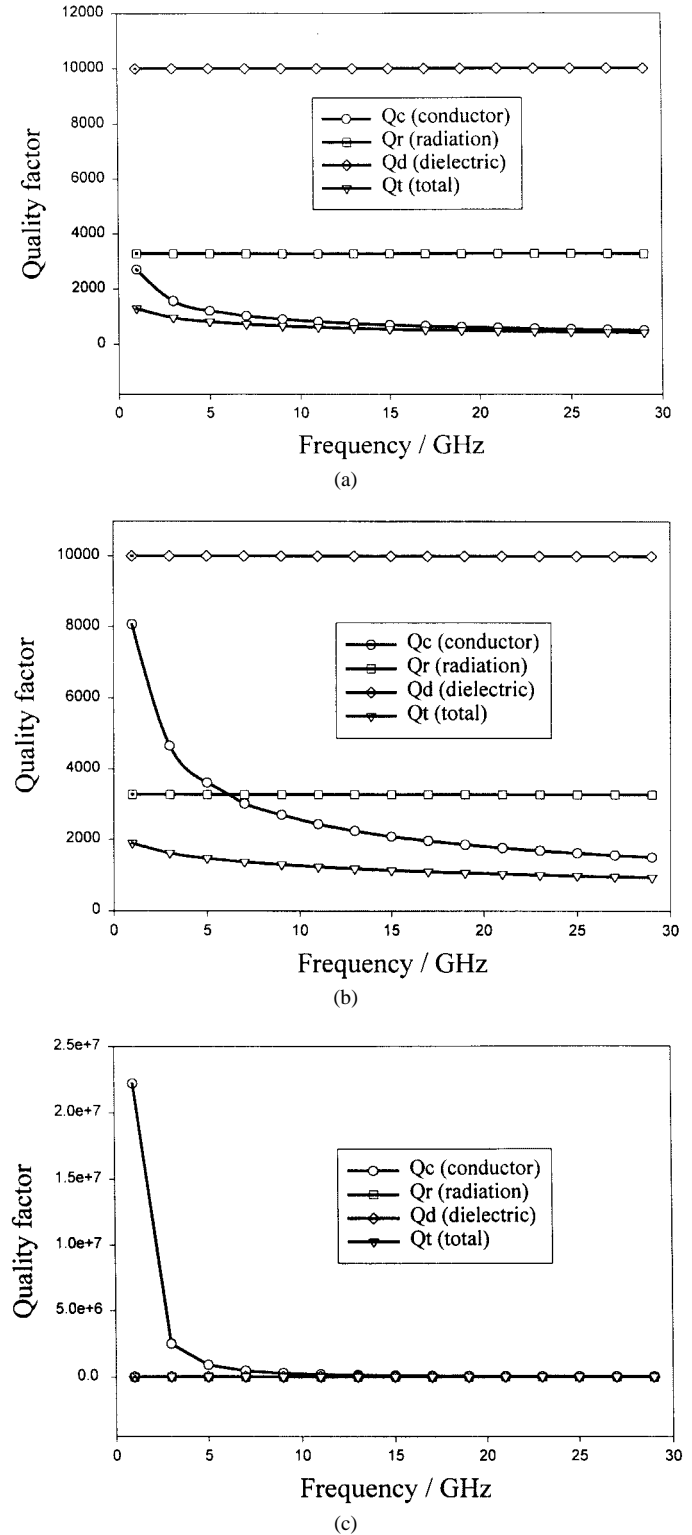

Fig. 9. The quality factors associated with the "H" antenna. Conductor, dielectric, and radiation quality factors are shown for (a) copper antenna at 300 K, (b) copper antenna at 77 K, and (c) YBCO antennas. The loss tangent for the substrate is 10^{-5}. Surface resistance are as given in Fig. 6.

In general, the electric potential at a point $\underline{r}$ is given by

$$\underline{F}(r) = \frac{\varepsilon_0}{4\pi} \int \int \underline{M}(r') \frac{\exp(-jk_0|r - r'|)}{|r - r'|} \, dS'. \qquad (2)$$

This integration is around the perimeter of the patch and inside the dielectric. Electric and magnetic fields in the farfield
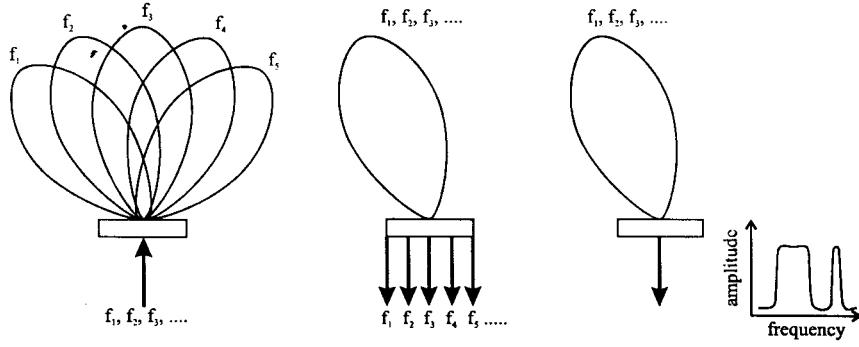
Fig. 10. Three functions of the HTS antenna array.

zone are then given by

$$\underline{H}(r) = -j\omega\underline{F}(r)$$
$$E_\theta(r) = \sqrt{\frac{\mu_0}{\varepsilon_0}}H_\phi(r) \tag{3}$$
$$E_\phi(r) = -\sqrt{\frac{\mu_0}{\varepsilon_0}}H_\theta(r).$$

This method of calculating the farfield radiation pattern requires the assumption of the current distribution. As a first estimate, assume that the electric field $\underline{E}_t$ has only a linear variation on each side of the "H" of the antenna. This assumption is later justified by the good agreement of this method with other results. An expression can thus be written down as

$$E_z = \frac{2xE_1}{e} + \frac{x}{|x|}\frac{2|y|E_0}{a}. \tag{4}$$

a and e are the width and length of the antenna defined in Fig. 1, and E_1 and E_0 are fields which define the rate of increase of the assumed linear increase of electric field of the patch. Using this value of electric field an analytical solution for the electric potential of a "H" antenna can be calculated

$$H_\theta(r,\theta,\phi) = H_x(r,\theta,\phi)\cos(\phi)\cos(\theta)$$
$$+ H_y(r,\theta,\phi)\sin(\phi)\cos(\theta)$$
$$H_\phi(r,\theta,\phi) = -H_x(r,\theta,\phi)\sin(\phi) + H_y(r,\theta,\phi)\cos(\phi) \tag{5}$$

where

$$H_x(r,\theta,\phi)$$
$$= \frac{4j\omega\varepsilon_0}{\pi r}\exp(-jk_0 r)\frac{\sin\left(k_0\cos(\theta)\frac{t}{2}\right)}{k_0\cos(\theta)}$$
$$\times \left\{ \frac{E_1}{C_1^2 C_3}[F1(C_1 C_3) - F2(C_1 C_3) \right.$$
$$- F1(C_1 C_4) + F2(C_1 C_4)]F1(C_2 C_5)$$
$$+ \frac{E_1}{C_1^2 C_3}[F1(C_1 C_4) - F2(C_1 C_4)]F1(C_2 C_6)$$
$$- \frac{E_0}{C_1}[F3(C_1 C_3) - F3(C_1 C_4)]F1(C_2 C_5)$$
$$\left. - \frac{E_0 C_6}{C_1 C_5}[F3(C_1 C_4) - 1]F1(C_2 C_6) \right\} \tag{6}$$

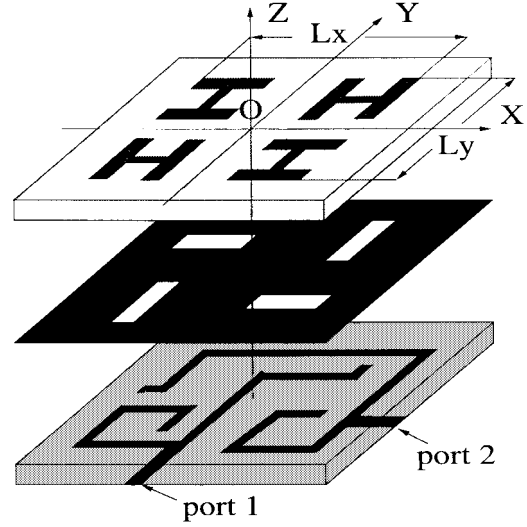Fig. 11. Four-element antenna array.

and

$$H_y(r,\theta,\phi)$$
$$= \frac{4j\omega\varepsilon_0}{\pi r}\exp(-jk_0 r)\frac{\sin\left(k_0\cos(\theta)\frac{t}{2}\right)}{k_0\cos(\theta)}$$
$$\times \left\{ \frac{E_1}{C_2}F1(C_2 C_5)F3(C_1 C_3) \right.$$
$$- \frac{E_1 C_4}{C_2 C_3}[F1(C_2 C_5) - F1(C_2 C_6)]F3(C_1 C_4)$$
$$+ \frac{E_0}{C_2^2 C_5}[F3(C_2 C_5) + C_2 C_5 F1(C_2 C_5) - 1]$$
$$\times F3(C_1 C_3) - \frac{E_0}{C_2^2 C_5}[F3(C_2 C_5)$$
$$+ C_2 C_5 F1(C_2 C_5) - F3(C_2 C_6)$$
$$\left. - C_2 C_6 F1(C_2 C_6)]F3(C_1 C_4) \right\} \tag{7}$$

with

$$F1(x) = \sin(x), \quad F2(x) = x\cos(x), \quad F3(x) = \cos(x)$$
$$C_1 = \sin(\theta)\cos(\phi)k_0, \quad C_2 = \sin(\theta)\sin(\phi)k_0$$
$$C_3 = 0.5e, \quad C_4 = 0.5c, \quad C_5 = 0.5a, \quad C_6 = 0.5d.$$

Fig. 5 shows the radiation pattern of the "H" antenna using the above expressions. This radiation pattern is compared with full-wave analysis and experimental measurements.

D. Efficiency

The efficiency of the antenna can be calculated by considering losses. The input power to the antenna is dissipated in: 1) the conductor making up the antenna (P_c); 2) the power dissipated in the dielectric (P_d); and 3) power radiated (P_r). These can be calculated from the electromagnetic fields by

$$P_d = \frac{\omega \varepsilon \delta}{2} \int \int \int |E_z|^2 \, dv \qquad (8)$$

$$P_c = R_s \int \int |\underline{H}|^2 \, ds \qquad (9)$$

$$P_r = \frac{1}{4} \sqrt{\frac{\varepsilon_0}{\mu_0}} \int_0^{2\pi} \int_0^{\pi} |\underline{E}|^2 r^2 \sin(\theta) \, d\theta \, d\phi. \qquad (10)$$

The losses in both copper and superconducting antennas are shown in Fig. 6 as a function of frequency. All dimensions, including the substrate thickness, are assumed to scale with frequency and normalized to the antenna dimensions given above at a frequency of 4.5 GHz. A loss tangent of the substrate material of 10^{-5} is used in the calculation. Values of $E_1 = 0.2$ and $E_0 = 0.8$ are chosen in the example below. These particular values are deduced from the field distribution shown in Fig. 4(b). As can be observed, the conductor losses increase with frequency but are much less for the superconducting antenna.

Surface wave loss is not important if the dielectric thickness is less than about one-tenth of a free space wavelength [17]. The efficiency of the antenna is simply given by

$$e = \frac{P_r}{P_r + P_d + P_c}. \qquad (11)$$

The efficiency as a function of frequency is shown in Fig. 7, and the same parameters are used as those in Fig. 6. The improvement in efficiency, especially at higher frequencies, for the YBCO antenna is self-evident. The main losses contributing to the efficiency of the HTS antenna in Fig. 7 are the losses associated with the dielectric. Experimental results for both copper and superconducting antennas are also shown in the figure for comparison.

A further comparison of the above expression can be done by looking at the data obtained by Chaloupka in [9]. A method of moments analysis was done on the antenna structure to compute the efficiency, and experimental results were also included in the reference and are shown in Fig. 8. The efficiency increases as a function of the substrate thickness because the radiation increases. However, as seen in Fig. 8, there is a considerable difference between the efficiency of the copper and superconducting antennas. The values of $E_0 = 0.8$ and $E_1 = 0.2$ were deduced from a full wave analysis of the antenna structure with a thickness of 1.27 mm. These values do not change appreciably for different "H" antennas.
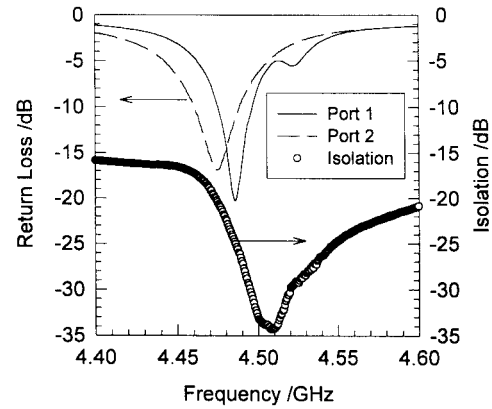

Fig. 12.   Measured return loss and isolation of the dual-band self-diplexing four-element "H" antenna array.
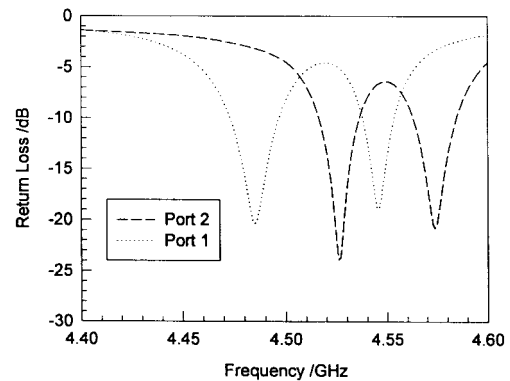

Fig. 13.   Four-frequency operation of the four element two port "H" antenna array.

E. Quality Factor

Finally, the quality factors of the antenna can be deduced. The dielectric, conductor, and radiation quality factors are given by

$$Q_d = \frac{\omega W}{P_d}, \qquad Q_c = \frac{\omega W}{P_c}, \qquad Q_r = \frac{\omega W}{P_r} \qquad (12)$$

where W is the total stored energy at resonance given by

$$W = \frac{\varepsilon}{2} \int \int \int |\underline{E}_z|^2 \, dv = \frac{P_d}{\omega \delta}. \qquad (13)$$

Fig. 9 shows the quality factors associated with the various antennas under discussion. The YBCO antenna has a much higher conductor quality factor then the copper antennas, as expected.

III. ANTENNA ARRAYS

In order to fully exploit the distinct advantages of small planar superconducting antennas they need to be included into antenna arrays. Fig. 10 shows three separate possible functions of an HTS antenna array. Fig. 10(a) shows diagrammatically how the array can produce a number of separate radiation patterns, the radiation pattern produced being dependent upon the frequency of the input signal. The same type of array can act as a channelizer as depicted in Fig. 10(b). Here the
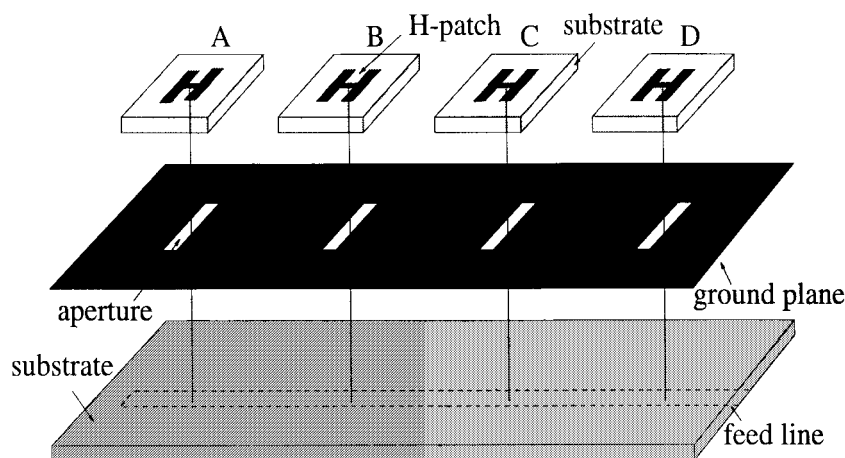
Fig. 14. Series fed "H" antenna array.

output of the antenna array has a number of ports, and the port that a signal emerges from depends upon the frequency of the received signal. The construction of separate channelizers as post processors has been the topic of many research investigations, and many different types of technology have been studied for this application in the past. The third use of the array is shown in Fig. 10(c); it can be configured as a front-end filter. Here filtering of an incoming signal can be accomplished in the antenna array itself. This can be simply used to increase the bandwidth of the array or perform a more complicated filtering action. In addition, the polarization of any of the elements in the array can be controlled by the feed network and element orientation. With correct design, any of these three functions can be combined to form a multifunction array. An additional advantage is that the whole multifrequency antenna array is of a similar size to a conventionally designed antenna array operating at only a single frequency.

In the proposed arrays, the antennas are close together, and if they operate at the same frequency could interact strongly. However, because they are at different frequencies, the interaction becomes less of a problem and this will aid the design considerably. Alternatively, if the antennas are at the same frequency the orientation of the individual antennas can be changed to reduce mutual coupling. Below we discuss three practical examples that relate to each of the concepts shown in Fig. 10.

A. Dual-Band Self-Diplexing Four-Element "H" Antenna Array

Fig. 11 shows the arrangement of a four-element antenna array; the size of this array is about the same as a single square microstrip patch antenna. By using an appropriate feed network, this array can be configured for a number of functions [15]. By using two of the antennas connected in series at one frequency and two at another frequency, the array can be used to produce an array that acts as a diplexer. Additional isolation between the ports is obtained because the polarization is mutually orthogonal as the "H" antennas are normal to each other.

Fig. 12 shows the return loss for each of the two inputs and the isolation between the two channels. The isolation is good

and is dominated by cross coupling in the feed network. It can be improved by using thinner substrates. The 10-dB bandwidth is 0.6%, small as expected for this antenna. In addition, the same feed network can provide a four-frequency operation; the return loss of an example network is shown in Fig. 13. In this case, there are two ports, but each of the four "H" antennas operates at a different frequency.

This four-element array can also be configured as two circular polarized antennas by changing the feed network if two of the orthogonal antennas are fed by a signal 90° out of phase circular polarization results.

B. Four-Element Series Array

A series array is shown in Fig. 14. In this case, there is a single feed point, and with the appropriate "H" antenna configuration a number of interesting functions can be produced.

Fig. 15 shows the return loss for three examples of how this type of antenna array may be used. Fig. 15(a) shows how the array may be used for four separate frequencies, the bandwidth being dependent upon the antenna element itself. Fig. 15(b) shows how the bandwidth of the antenna may be increased, and this time the array has two frequencies of operation; each operating frequency has an increased bandwidth due to the use of two "H" antennas. If a single frequency of operation is required with extended bandwidth, this is obtained by using a larger number of antennas of close operating frequency. Fig. 15(c) shows the return loss of a wider band antenna array.

C. Six-Element Array for Dual-Beam Dual-Frequency Operation

Fig. 16 shows the feed network of dual-beam dual-frequency antenna array, with the position of the "H" antenna shown as dotted lines. The array produced two beams at ±30° from the normal. One beam operates at 8 GHz and the other 12 GHz. The feed network was designed using Hewlett Packard MDS. The 50-Ω input transmission line is first split and radial stubs are used to block the appropriate frequency. The feeds for both 8 and 12 GHz are then split using the appropriate impedance transmission lines, resulting in 75-Ω transmission lines to feed the "H" antenna.

Fig. 16. The feed network for a dual-beam dual-frequency antenna array. The "H" elements are shown as dotted lines.
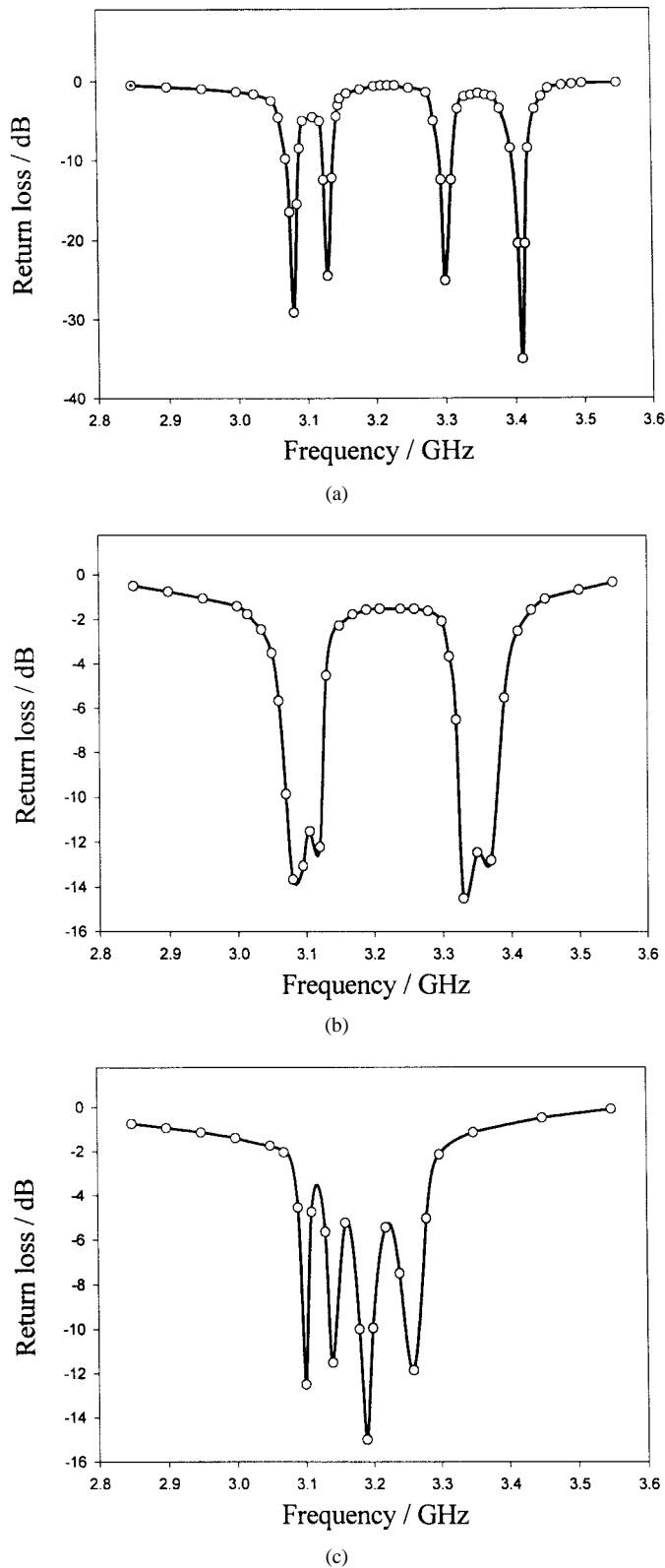

Fig. 15. Return loss of a four-element series-fed antenna array. (a) Multi-frequency operation, (b) two-frequency operation with extended bandwidth, and (c) Wider band operation.
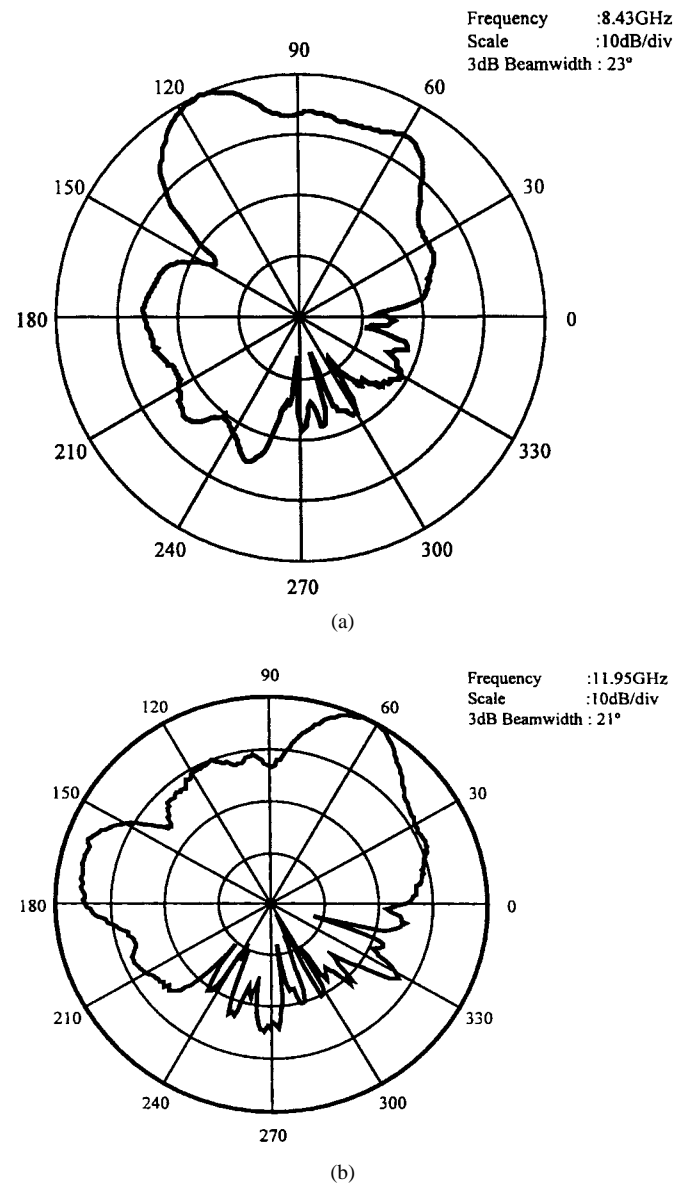
Fig. 17. Radiation patterns from the dual-beam, dual-frequency, six-element antenna array. (a) 8 GHz. (b) 12 GHz.

The radiation patterns of the arrays are shown in Fig. 17. The beam directions are about 30° to the normal in both cases and have low directivity. The two main beams have about a 10-dB larger level than t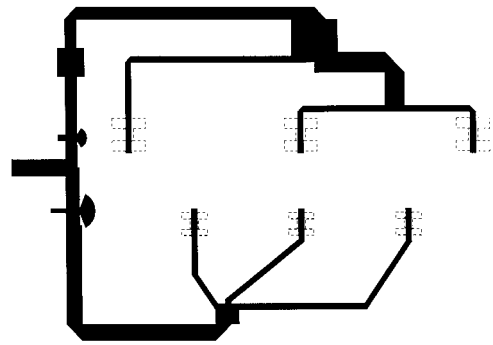he background; this is expected from an array with such a small number of elements. The efficiency of both arrays has been measured at about 10% when they are made in copper.

IV. CONCLUSION

In almost all practical applications of superconducting antenna, arrays will be used. The "H" antenna is a suitable candidate for inclusion in multifunction arrays. The "H" element is about the size of a standard square patch antenna and its efficiency can be considerably improved when used in its superconducting form. Arrays with multifunction capability are considerably easier to design if several antennas can be enclosed in an area of a subwavelength square. Such arrays can have functions of channelization, front end filtering, and multibeam and diverse polarization capability.

ACKNOWLEDGMENT

REFERENCES

[1] S. K. Khamas, M. J. Mehler, T. S. M. Maclean, C. E. Gough, N. McN. Alford, and M. M. Harmer, "High-T_c superconducting short dipole antenna," *Electron. Lett.*, vol. 24, no. 8, pp. 460–461, 1988.
[2] M. J. Lancaster, *Passive Microwave Device Applications of High Temperature Superconductors*. Cambridge, U.K.: Cambridge Univ. Press, 1997.
[3] H. Chaloupka, "High temperature superconductor antennas: Utilization of low RF losses and of nonlinear effects," *J. Superconduct.*, vol. 5, no. 4, pp. 403–416, 1992.
[4] ———, "Superconducting multiport antenna arrays," *Microwave Opt. Technol. Lett.*, vol. 6, no. 13, pp. 737–744, 1993.
[5] J. S. Herd, D. Hayes, J. P. Kenney, L. D. Poles, K. G. Herd, and W. G. Lyons, "Experimental results on a scanned beam microstrip antenna array with a proximity coupled YBCO feed network," *IEEE Trans. Appl. Superconduct.*, vol. 3, pp. 2840–2843, 1993.
[6] M. A. Richard, K. B. Bhasin, C. Gilbert, S. Metzler, G. Koepf, and P. C. Claspy, "Performance of a four-element Ka-band high-temperature superconducting microstrip antenna," *IEEE Microwave Guided Wave Lett.*, vol. 2, pp. 143–145, 1992.
[7] M. A. Richard, K. B. Bhasin, and P. C. Claspy, "Superconducting microstrip antennas: An experimental comparison of two feeding methods," *IEEE Trans. Antennas Propagat.*, vol. 41, pp. 967–974, 1993.
[8] V. Palanisamy and R. Garg, "Rectangular ring and H shaped microstrip antennas—Alternatives to rectangular patch antennas," *Electron. Lett.*, vol. 21, no. 19, pp. 874–876, 1985.
[9] H. Chaloupka, N. K. Llein, M. Peinger, H. Piel, A. Pischke, and G. Splitt, "Miniaturised high-temperature superconductor microstrip patch antenna," *IEEE Trans. Microwave Theory Tech.*, vol. 39, pp. 1513–1521, 1991.
[10] A. Pischke, H. Chaloupka, H. Piel, and G. Splitt, "Electrically small planar HTS antennas," in *Proc. 3rd Int. Superconductive Electronics Conf.*, Univ. of Strathclyde, U.K., June 1991, pp. 340–343.
[11] A. M. Portis, H. Chaloupka, M. Jeck, H. Piel, and A. Pischke, "Critical response of an HTS microstrip patch antenna," in *Proc. 3rd Int. Superconductive Electronics Conf.*, Univ. of Strathclyde, U.K., June 1991, pp. 320–324.
[12] A. M. Portis, H. Chaloupka, and M. Jeck, "Power induced switching of an HTS microstrip patch antenna," *Superconductor Sci. Technol.*, vol. 4, pp. 436–438, 1991.
[13] J. S. Hong and M. J. Lancaster, "Microstrip H-shaped antenna aperture coupled to a microstrip feed line," in *Proc. 26th European Microwave Conf.*, Prague, Czech Republic, Sept. 9–12, 1996, pp. 284–287.
[14] H. Y. Wang, J. S. Hong, and M. J. Lancaster, "Aperture coupled high-temperature superconductor microstrip small antennas," in *Proc. European Conf. Applied Superconductivity*, 1997, paper 3Ge-7, pp. 359–362.
[15] J. S. Hong and M. J. Lancaster, "Experimental investigation of aperture-coupled four-element microstrip H-shaped antenna for multi-function operation," in *Proc. 10th Int. Conf. Antennas and Propagation*, Apr. 14–17, 1997, pp. 1.78–1.81.
[16] B. C. Wadell, *Transmission Line Design Handbook*. Norwood, MA: Artech, 1991.
[17] J. R. James and P. S. Hall, *Handbook of Microstrip Antennas*. London, U.K.: Peter Peregrinus, 1989.

Michael J. Lancaster (M'91) received the physics degree in 1980 and a Ph.D. degree in research into nonlinear underwater acoustics in 1984, both from Bath University, U.K.

After leaving Bath University he joined the Surface Acoustic Wave (SAW) group at the Department of Engineering Science, Oxford University, as a Research Fellow. The research was in the design of new, novel SAW devices, including filters and filter banks. In 1987 he became a Lecturer at The University of Birmingham in the School of Electronic and Electrical Engineering, lecturing in electromagnetic theory and microwave engineering. Shortly after he joined the school he began the study of the science and applications of high-temperature superconductors, working mainly at microwave frequencies. Currently he heads the Electronic and Materials Devices group as a Reader. His research interests include microwave filters and antennas, as well as the high-frequency properties and applications of a number of novel and diverse materials.

Dr. Lancaster is currently serving on the IEEE Microwave Theory and Techniques Society's International Microwave Symposium Technical Committee.

Hanyang Y. Wang received the M.Eng. degree from Northwestern Polytechnic University, Xian, China, in 1986 and the Ph.D. degree from Heriot-Watt University, Edinburgh, U.K., in 1995.

From 1986 to 1991, he was employed at the Department of Electronic Engineering of Shandong University, Jinan, China, where he served as an Assistant Lecturer, Lecturer, and Associated Professor. From 1995 to 1997, he was a Senior Research Officer in the Department of Electronic System Engineering, the University of Essex, Colchester, U.K. He is currently a Research Fellow in the School of Electrical and Electronic Engineering, the University of Birmingham, Birmingham, U.K. His research interests include microwave devices for communications, antennas and antenna array, superconducting antennas, and numerical methods for the solutions of electromagnetic radiation and scattering problems. He is the author of over 40 scientific papers on these topics.

Jia-Sheng Hong (M'94) received the D.Phil. degree in engineering science from Oxford University, U.K., in 1994.

From 1979 to 1983 he worked at Fuzhou University as a Teaching/Research Assistant in radio engineering. He then visited Karlsruhe University, Germany, where he worked on microwave and millimeter-wave techniques from 1984 to 1985. In 1986 he returned to Fuzhou University as a Lecturer in microwave communications. In 1990 he was awarded a K. C. Wong Scholarship by Oxford University and became a graduate member of St. Peter's College at Oxford University, where he conducted research in electromagnetic theory and applications. Since 1994 he has been a Research Fellow at Birmingham University, U.K. His current interests include RF and microwave devices for communications, microwave filters and antennas, microwave applications of high temperature superconductors, electromagnetic modeling, and the genetic approach for signal processing and optimization.

In 1983 Dr. Hong was awarded a Friedrich Ebert Scholarship.